

This item is the archived peer-reviewed author-version of:

Time-optimal bang-bang driven rest-to-rest motion through an angular switching point

Reference:

Ceulemans David, Van Oosterwyck Nick, De Viaene Jasper, Steckel Jan, Derammelaere Stijn.- Time-optimal bang-bang driven rest-to-rest motion through an angular switching point
2022 IEEE/ASME International Conference on Advanced Intelligent Mechatronics (AIM), 11-15 July, 2022, Sapporo, Japan - ISSN 2159-6255 - 2022, p. 1639-1645

Full text (Publisher's DOI): <https://doi.org/10.1109/AIM52237.2022.9863247>

To cite this reference: <https://hdl.handle.net/10067/1901210151162165141>

Time-optimal bang-bang driven rest-to-rest motion through an angular switching point

David Ceulemans^{1,4}, Nick Van Oosterwyck^{1,4}, Jasper De Viaene^{2,5}, Jan Steckel^{3,4} and Stijn Derammelaere^{1,4}

Abstract— For economic reasons, machine builders are increasingly challenged to make single-axis driven machines perform rest-to-rest movements as fast as possible over time. In terms of control, a time-optimal motion is performed by injecting a bang-bang torque profile, characterized by a discrete switching point. However, the state-of-the-art to obtain the ideal application-dependent switching point is often computationally demanding and lacks robustness, hampering smooth system implementation. Moreover, machine builders invariably design their machines using CAD software, which automatically provides good knowledge about, e.g., the machine’s load torque profile. Therefore, in this work, based on Newton’s work-energy principle, a framework for variable inertia systems is derived and used as a starting point to estimate the optimal bang-bang switching point efficiently, employing CAD extracted data. In addition, a self-learning control structure is proposed to correct for the initial switching point so that the application continues to move time-optimally, regardless of system influences such as temperature variation. A case study is used to validate the proposed methodology and associated control structure through simulation.

I. INTRODUCTION

Numerous industrial applications are characterised by a repetitive motion consisting of a single degree of freedom (1-DOF) forward and backward rotation, e.g. pick-and-place units, weaving machines, etc. Typically, these motion applications only constrain a fixed start θ_{start} and end angle θ_{end} , and demand that the application stand still at either angle. This is often referred to as point-to-point or rest-to-rest (RtR) movements in the literature. The limited number of trajectory constraints implies that machine builders have the freedom to shape the intermediate motion profile as desired. This enables the possibility to assign preferable properties to the eventual motion profile, such as minimal required energy to move along the trajectory [1], a limited maximal motor torque [2], or a minimal motion time [3]. The latter is the focus of this work.

¹David Ceulemans, Nick Van Oosterwyck and Stijn Derammelaere are with the Departement of Electromechanics, CoSysLab, University of Antwerp, Groenenborgerlaan 171, 2020 Antwerp, Belgium (email: david.ceulemans@uantwerp.be; nick.vanoosterwyck@uantwerp.be; stijn.derammelaere@uantwerp.be)

²Jasper De Viaene is with the Department of Electrical Energy, Metals, Mechanical Constructions and Systems, University of Ghent campus Kortrijk, Belgium (email: jasper.deviae@ugent.be)

³Jan Steckel is with the Department of Electronics, CoSysLab, University of Antwerp, Groenenborgerlaan 171, 2020 Antwerp, Belgium (email: jan.steckel@uantwerp.be)

⁴David Ceulemans, Nick Van Oosterwyck, Stijn Derammelaere and Jan Steckel are with AnSyMo/CoSys, Flanders Make, the strategic research centre for the manufacturing industry

⁵Jasper De Viaene is with EEDT-MP, Flanders Make, the strategic research centre for the manufacturing industry

A minimum motion time for industrial mechanisms has been the subject of research for many years. In order to move a rotary machine from a start θ_{start} to an end angle θ_{end} as fast as possible (ASAP), it is intuitive to first apply maximum acceleration with maximum torque T_{max} until a certain switch point t_{SwP} , followed by maximum deceleration until the end angle θ_{end} is reached. In the literature, there is a consensus that mathematically, for scalar linear systems in the continuous-time domain to evolve ASAP, the optimal system’s input torque $T(t)$ should be as large as possible and is described as being of the form bang-bang (see Fig. 2) [4]–[6]. The exact timing of the switching point t_{SwP} between maximal positive and maximal negative motor torque T_{max} is a complex matter, especially analytically [7]. Therefore, all recent literature determines the optimal switching point $t_{SwP;Opt}$ numerically based on dynamic equations, e.g., forward and backward integration [8], [9], which can be computationally challenging. Especially since, depending on the application, inertia J , load torque T_l , damping b , stiffness k , and friction b_l can change as a function of the motor’s rotor angle θ . Already in [5], the idea of a phase-plane was introduced to determine the optimal switching point $t_{SwP;Opt}$ between the two motion primitives. A mathematical characterization is given in [6] for a minimum-time rest-to-rest motion of a generic non-flexible linear scalar system (being bang-bang), taking into account system constraints. [7] characterized the optimal bang-bang control approach for a damped flexible system (minimum one flexible mode) and concluded that to achieve a time-optimal motion without residual vibrations, multiple bang-bang switches are required. Subject to the damping ratio, for a single flexible mode system, the location of the additional switches varies between near the middle or at the end of the trajectory. Moreover, the number of switches can vary. The switching pattern of undamped systems is also found to have periodic properties [4], which contributes to a computationally simplified online implementation. Model predictive control approaches were proposed in [10], [11], which have the main advantage of reacting adaptively to setpoint changes during a movement. Nevertheless, they require in-situ tuning before commissioning.

In theory, as far as implementation is concerned, a pure torque controller should suffice. However, since all previous methods are affected by model uncertainties such as motor cogging, an additional active controller is often required to eliminate a final residual error θ_{error} . Practical implementation of an optimal bang-bang profile can be divided into two implementation strategies: a cascade control with time-optimal

commands in the feedforward or a pure torque control followed by a pure cascade control over time [1], [4]. Still, the reviewed methods to obtain time-optimal control remain computationally demanding regardless of their need for mechanisms to correct model uncertainties. As an alternative, [12] proposed to combine a model-independent iterative learning control approach with a bi-section algorithm to determine an in-situ time-optimal movement. However, despite easy implementation, the convergence towards the optimum should be slower than with model-based methods.

This work tries to overcome the aforementioned hurdles by combining a good computationally friendly first initial guess of the optimal bang-bang timing with a self-learning correction mechanism. Machine builders often design their applications using, e.g., CAD software, which automatically provides basic information about the application such as the load torque $T_l(\theta)$ or the machine inertia $J(\theta)$ [1]. In this work, a proper initial timing of the bang-bang switching point is no longer determined in the time t_{SwP} , but in the angular domain θ_{SwP} , based solely on the CAD load torque $T_l(\theta)$ and Newton's energy theorem for a single rigid body. Moreover, the idea is embraced that self-learning online correction mechanisms remain necessary for a time-optimal movement. Therefore, a simple self-learning algorithm based on the residual error θ_{error} is proposed to correct model uncertainties and unmodeled effects.

The remainder of this work is structured as follows. In section II-A, an equilibrium equation is derived for variable inertia single-mass systems starting from Newton's work-energy principle. Based on this equilibrium, a formula is derived in section II-B that allows the calculation of the optimal switching point $\theta_{SwP;Opt}$. In chapter III, a control structure is proposed based on the introduced switching point θ_{SwP} . Finally, chapter IV validates the proposed concept in simulation using an application represented by a two-mass model.

II. THEORETICAL DERIVATION OF THE OPTIMAL REST-TO-REST SWITCHING POINT θ_{SwP}

A. Derivation of the work-energy principle for a single-mass variable inertia rigid body

Consider a single-mass rigid body, as shown in Fig. 1, which inertia $J(\theta)$ varies as a function of its rotation angle $\theta(t)$. The behaviour of this type of system is representative of many industrial applications. The rotation is initiated by a resultant net torque $T(t)$, which is the vectorial sum of both the driving torque $T_{motor}(t)$ and the load torque $T_l(t)$. In addition, the body may be subject to friction $T_b(t)$. For the time being, the latter will be neglected, assuming that the torque loss due to friction is insignificant compared to the total motor torque $T_{motor}(t) \gg T_b(t)$ [13].

Starting from the Euler-Lagrange equation, a formulation can be derived describing the relation between the resulting net torque $T(t)$ and the body's angular position $\theta(t)$, speed $\omega(t)$ and acceleration $\alpha(t)$ [14]:

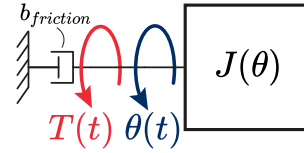


Fig. 1. General representation of system consisting of a single-mass rigid body, subject to rotation $\theta(t)$ caused by the resultant torque $T(t)$.

$$T(t) = J(\theta(t)) \cdot \alpha(t) + \frac{1}{2} \frac{d(J(\theta(t)))}{d(\theta(t))} \cdot \omega^2(t). \quad (1)$$

Next, Newton's work-energy theorem is considered. The theorem states that a change in the rigid body's kinetic energy is equal to the work done by external forces acting on that body [15], [16]. Given the mechanism described by equation (1), in what follows, the relationship is derived between the work performed by an external torque $T(t)$ acting on a rigid body system and the change in kinetic body's energy. The total work done by external forces from time t_1 to t_2 , acting on a 1-DOF rotating rigid body, can be calculated following:

$$W = \int_{t_1}^{t_2} \left(\vec{T}(t) \cdot \vec{\omega}(t) \right) dt. \quad (2)$$

Since the torque $\vec{T}(t)$ and the rotation vector $\vec{\omega}(t)$ are in line, the vectorial character is omitted in the sequel. On the one hand, equation (2) can be rewritten as:

$$W = \int_{t_1}^{t_2} \left(T(t) \cdot \omega(t) \right) dt = \int_P \left(T(\theta(t)) \right) d(\theta(t)), \quad (3)$$

given that P is the path from $\theta(t_1)$ to $\theta(t_2)$. Since the scalar product of torque T and rotational speed ω should be evaluated along a position trajectory, the integral is considered as a line integral. On the other hand, by substituting equation (1) into equation (2), equation (2) can be rewritten as:

$$W = \int_{t_1}^{t_2} \left(\left(J(\theta) \cdot \alpha(t) + \frac{1}{2} \frac{d(J(\theta(t)))}{d(\theta(t))} \cdot \omega^2(t) \right) \cdot \omega(t) \right) dt. \quad (4)$$

By further elaborating equation (4) (see appendix I), one can prove that the work done by the considered single-mass system can be calculated following

$$W = \frac{J(\theta(t_2)) \cdot \omega(t_2)}{2} - \frac{J(\theta(t_1)) \cdot \omega(t_1)}{2}. \quad (5)$$

And finally, by equating both expanded formulations (3) and (5), one obtains:

$$\int_P \left(T(\theta(t)) \right) d(\theta(t)) = \frac{J(\theta(t_2)) \cdot \omega(t_2)}{2} - \frac{J(\theta(t_1)) \cdot \omega(t_1)}{2}. \quad (6)$$

Equation (6) describes the relationship between the work exerted on the system by an external torque $T(\theta)$ and the kinetic energy of the single-mass system. Starting from equation (6), a formula to analytically calculate the optimal switching point $\theta_{SwP;Opt}$ is elaborated in section II-B.

B. Derivation of the optimal switching point for a bang-bang driven rest-to-rest motion profile

This work aims to make a system perform a time-optimal RtR movement as quickly as possible from a start angle θ_{start} to an end angle θ_{end} . To achieve this, as shown in Fig. 2, the literature previously showed that the torque profile's shape should be of the form bang-bang with one discrete switch between maximal positive and negative injected motor torque T_{max} . In what follows, the optimal point to switch in the angular domain $\theta_{SwP;Opt}$ is analytically determined. Non-optimal switching leads, as shown in Fig. 2, to an undesired application standstill at an angle either smaller or larger than the desired end angle θ_{end}^* .

To determine the optimal switching point $\theta_{SwP;Opt}$ analytically, equation (6) is used as a starting point, which is the work-energy relation for single rigid body systems with position-dependent inertia. Moreover, given the desire to move from a rest to a rest position, the start and end angle speed $\omega(t)$ at time t_1 and t_2 are equal to zero. Therefore, the integral of the net external torque $T(\theta)$ acting on our system along the path θ_1 to θ_2 equals 0:

$$\int_P \left(T(\theta(t)) \right) d(\theta(t)) = 0. \quad (7)$$

Equation (7) is further elaborated in the appendix (II) so that finally, for a bang-bang torque driven rest-to-rest motion profile, the optimal switching point angle $\theta_{SwP;Opt}$ can be calculated following

$$\theta_{SwP;Opt} = \frac{T_{max} \cdot (\theta_{start} + \theta_{end}) + \int_{\theta_{start}}^{\theta_{end}} (T_l(\theta)) d(\theta)}{2 \cdot T_{max}}, \quad (8)$$

with T_{max} the maximal motor torque and $T_l(\theta)$ the load torque of the considered mechanism. Note that the optimal switching point $\theta_{SwP;Opt}$ is inertia J independent, even in the case where inertia J varies as a function of rotor angle/position θ .

III. IMPLEMENTATION OF AN ANGULAR SWITCHING POINT θ_{SwP} DETERMINED BANG-BANG DRIVEN REST-TO-REST MOTION

A. Angular switching point controller for an idealized single-mass rigid body

An appropriate control structure is required to achieve a time-optimal motion using an angular switching point θ_{SwP} . For an idealized single-mass model, in this work, the control structure shown in Fig. 3 is proposed, consisting of a pure torque controller responsible for the injection of the bang-bang torque profile followed by a classical cascade control [17] to maintain the end angle θ_{end} . First, the torque controller desires a maximum positive torque T_{max} value from the starting angle θ_{start} of the trajectory until the switching point θ_{SwP} . After this point, maximum negative torque is desired until the end position θ_{end} , or to the point where the speed ω changes sign $\theta_{sng(\omega) \neq c^e}$. In an ideal scenario, assuming an optimal switch point $\theta_{SwP;Opt}$, both these points θ_{end} and $\theta_{sng(\omega) \neq c^e}$

should be equal to the desired end angle θ_{end}^* . Hence, when the end angle θ_{end} is reached, the motor's rotor speed ω should equal zero. The cascade controller serves purely to maintain the desired end angle θ_{end}^* .

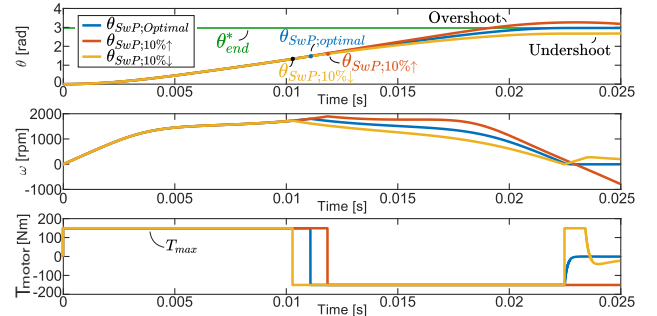


Fig. 2. Illustration of the position trajectory for an optimal switching point value $\theta_{SwP;Opt}$ (blue), a too large switching point value θ_{SwP} (orange) and a too small switching point value θ_{SwP} (yellow).

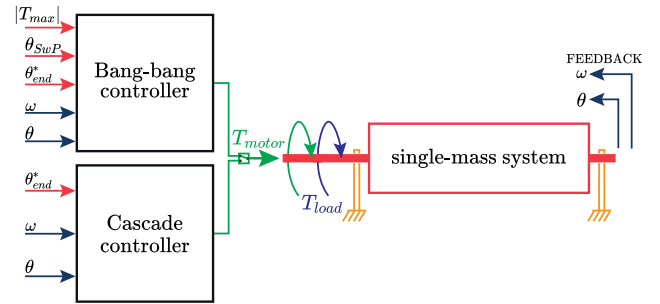


Fig. 3. Proposed control structure for a time-optimal rest-to-rest movement, consisting of a bang-bang torque controller and classic cascade controller.

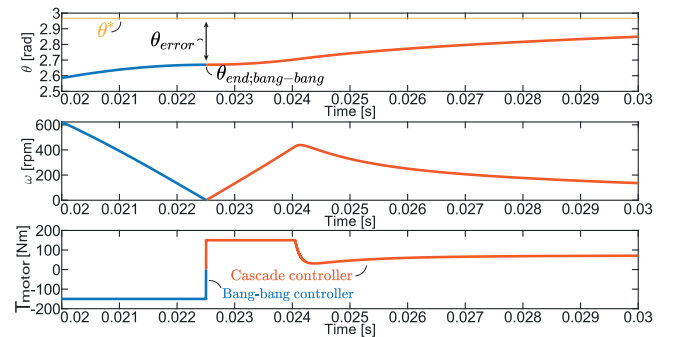


Fig. 4. Illustration of the switch between torque and cascade controller. The residual error that remains after the torque controller is eliminated by the cascade controller.

B. Non-idealized angular switching point controller

Section (III-A) assumes an idealised load consisting of a single rigid mass. Friction is neglected, and perfect knowledge of the application's load torque profile is required. Besides that, the motor torque T_{motor} is assumed to be constant

throughout the entire motor's operation range. The torque T_{motor} is presumed to change in value in infinitesimal time. And finally, the switching point θ_{SwP} calculation does not consider the time delays caused by, e.g., the processing of measured rotor angle θ in the motor controller. In reality, each of the aforementioned points should be taken into account to move in time optimally. For example, no matter how small, friction impacts the location of the optimal switching point $\theta_{SwP;Opt}$. Nevertheless, the effect of friction is challenging to model, especially its temperature dependency. Therefore, friction is challenging to include in the determination of the optimal switching point $\theta_{SwP;Opt}$. Given the foregoing, the exact analytical determination of the optimal switching point $\theta_{SwP;Opt}$ seems almost impossible, or would increase the analytical complexity drastically, hampering a computational-friendly implementation

Consequently, in practice, implementation purely based on a torque controller and a model determined switching point θ_{SwP}/t_{SwP} will always cause an error θ_{error} that requires compensation through, e.g., a cascade controller. However, the proposed switching point θ_{SwP} equation (8) can serve as a good approximate estimate of the true optimal switching point $\theta_{SwP;Opt}$. Fig. 4 illustrates the positioning correction of the cascade control following the bang-bang torque control motion $\theta_{end;bang-bang}$ for a situation where the desired end angle θ_{end}^* is not reached. In the proposed control structure shown in Fig. 3, switching between torque and cascade controller is based on one of the following triggers: exceeding the position setpoint θ_{end}^* or a change in the speed sign $sgn(\omega)$. In Fig. 4 the speed ω changes sign (the speed becomes negative), whereupon the cascade controller is activated.

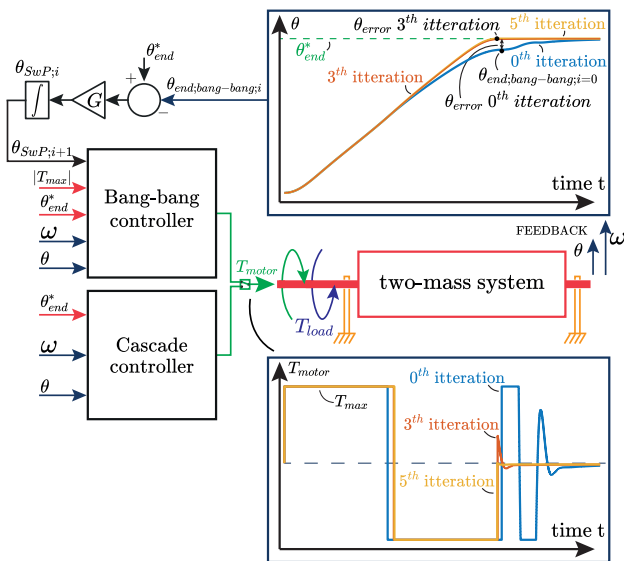


Fig. 5. Proposed control structure for a time-optimal rest-to-rest movement assuming an incompletely modelled two-mass system. Residual errors are compensated by iteratively updating the switching point θ_{SwP} .

C. Non-idealized self-learning switching point controller

Section III-B eliminates incomplete model residual error θ_{error} through a cascade controller. However, due to the repetitive nature of a rest-to-rest application, the calculated switching point θ_{SwP} will cause the same error between the desired end value θ_{end}^* and the actual bang-bang end position $\theta_{end;bang-bang}$ with each repetitive movement. Consequently, the same error θ_{error} must be compensated for every motion cycle, which leads to a permanent semi-time-optimal movement. In order to thoroughly compensate for this error θ_{error} , a straightforward self-learning mechanism is added to the earlier proposed control structure in Fig. 3. The idea behind the new self-learning control structure, presented in Fig. 5, is to adjust the switching point value θ_{SwP} after each iteration i by monitoring the machine's behaviour and thus minimizing the residual error θ_{error} shown in Fig. 4. In the end, the reduced error θ_{error} is a direct consequence of the improved timing of the bang-bang torque controller, which automatically results in an optimal motion time. The new switching point value for the next motion cycle $\theta_{SwP;i+1}$ is proposed to be calculated after each movement i using the current switching point value $\theta_{SwP;i}$, the residual error $\theta_{error} = \theta_{end}^* - \theta_{end;bang-bang;i}$ and a gain factor G following

$$\theta_{SwP;i+1} = \theta_{SwP;i} + (\theta_{end}^* - \theta_{end;bang-bang;i}) \cdot G. \quad (9)$$

IV. VALIDATION OF THE PROPOSED CONTROL STRUCTURE

Validation of the proposed methodology is performed by employing a case study. Both the ideal switching point bang-bang controller and the self-learning switching point control structure are validated in simulation using the presented case.

A. Mechanism under test

As a case, a mechanism represented by the two-mass spring-damper model shown in Fig. 6 is considered. The load with varying inertia $J_l(\theta_l)$ is driven via a rotor with inertia J_r . Both masses are linked via a coupling with spring constant k and damping factor b , both determined following the principle described in [18]. The machine properties, shown in Fig. 7, were extracted from CAD according to the procedure described in [1]. Finally, the friction coefficients of the motor b_r and load b_l are estimated. The machine properties of the non-position-dependent variables are summarised in table I. However, to validate the idealized switching point $\theta_{SwP;Opt}$ controller in the first place, the two-mass model is simplified to the single-mass model illustrated in Fig. 1. Friction is ignored, and the coupling between both masses is considered rigid so that $\theta = \theta_r = \theta_l$.

To validate the proposed control structures outlined in section III, the considered application is subjected to an ASAP motion with $\theta_{start} = 0$ rad and $\theta_{end} = 2.967$ rad (170°). Based on the load torque profile shown in Fig. 7, an initial switching point value θ_{SwP} of 1,4836 rad was found employing equation (8). The control parameters of the cascade control ($K_{p;position} = 801/s$, $K_{p;speed} = 36Nms/rad$, $T_{i;speed} = 1,2ms$) were set according to the methodology described in

[17]. The gain factor G from equation (9) was arbitrarily set at 0, 5.

TABLE I
MACHINE PROPERTIES OF THE CASE STUDY APPLICATION.

Motor			Coupling		Load
T_{max}	J_r	br	k	b	bl
[Nm]	[kg m ²]	[Nms/rad]	[Nm/rad]	[Nms/rad]	[Nms/rad]
150	0,0032	0,2	4221	0,396	0,1

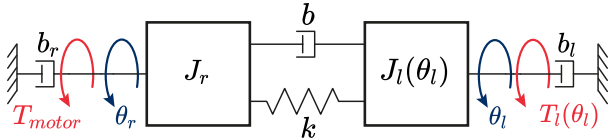


Fig. 6. The considered machine's conceptual representation consisting of a two-mass spring-damper model.

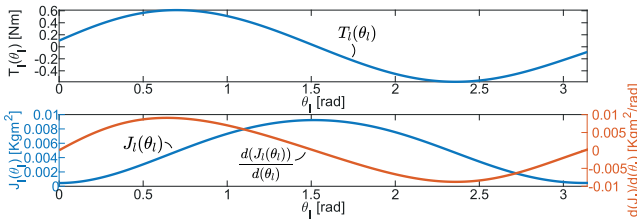


Fig. 7. CAD-extracted mechanical properties of considered machine: load torque T_l , inertia J_l and inertia variation $\frac{d(J_l)}{d(\theta_l)}$ as a function of the application angle θ_l .

B. Validation of the switching point controller for idealized situations

To validate the optimal switching point $\theta_{SwP;Opt}$ calculated following equation (8) and the accompanying controller from section (III-A), a simulation is performed in Matlab/Simulink using the single-mass model from IV-A. The simulation result, shown in blue in Fig. 2, proves that the optimal switching point $\theta_{SwP;Opt}$ results in a perfect rest-to-rest movement.

C. Validation of the self-learning switching point controller for non-idealized situations

To validate the self-learning control structure from III-C, both the controller and the two-mass system introduced in section IV-A were modeled. Since the model contains friction b_r , b_l and damping b , a residual error θ_{error} is expected. Fig. 8 visualizes the fifth iteration of the injected motor torque T_{motor} with the corresponding speed ω and position θ of both the motor rotor (in blue) and the application (in orange) over time. As shown in the position detail, the rotor position θ_r slightly fails to reach the requested end angle θ_{end}^* , whereupon the cascade control eliminates the remaining error θ_{error} . Furthermore, the velocity clearly shows that, due to the model's

flexible mode in combination with the absence of additional vibration eliminating bang-bang switches, the application is subject to residual vibrations when approaching the desired end angle θ_{end}^* . The magnitude and importance of these residual vibrations are, of course, application-dependent. If necessary, assuming a known motion profile, stiffness and damping of the system, a magnitude estimate of the residual vibrations can be made using the system's transfer function [19].

Moreover, Fig. 9 demonstrates the impact of the self-learning switching point $\theta_{SwP;i}$ as a function of the number of iterations i (motion cycles). Due to the friction present, the machine decelerates faster than would be the case without friction. Therefore, as intuitively expected, the switching point (angle) θ_{SwP} should evolve to a larger value (further in time) as initially calculated. Simulation results confirm that the eventual in-situ optimal angle to switch $\theta_{SwP;Opt}$ between acceleration and deceleration converges to a value larger than the initially calculated switching point θ_{SwP} , as shown in Fig. 9. To quantitatively evaluate the effect of the improved switching point $\theta_{SwP;i}$, the settling time t_{set} of both the motor position θ_r and the application θ_l are considered. A margin of error of $0,02^\circ$ was assumed. For the given machine, the simulation results show that, after eight iterations ($i = 8$), the motor reaches its desired end angle θ_{end}^* within 27ms given an error band of $\pm 0,01^\circ$. The application itself takes a little longer to damp out and, for the same tolerance limits, reaches its desired end angle θ_{end}^* after 33ms. So, in this case, the flexible mode amounts to a time delay of roughly 20%.

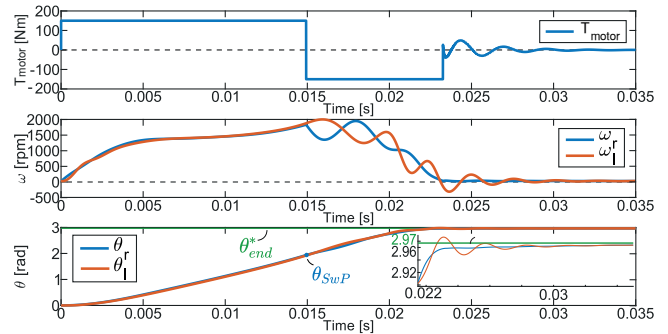


Fig. 8. The 5th iteration of the torque profile (top) with resulting position (bottom) and speed (middle) of both the motor and the application.

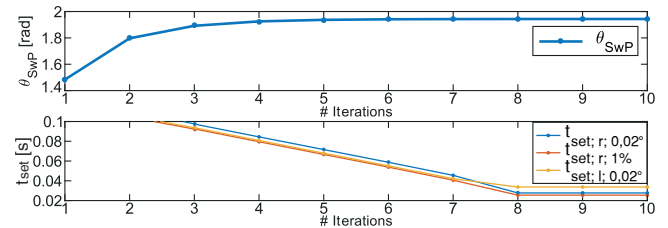


Fig. 9. The bang-bang switching point $\theta_{SwP;i}$ as a function of the number of iterations i performed (top). Settling time t_{set} of both the motor and application as a function of the updated switching point $\theta_{SwP;i}$ (bottom).

V. CONCLUSION

This work investigated the computationally efficient shaping of a bang-bang torque profile, characterized by a discrete switching point θ_{SwP} , to achieve a rotational application to perform a time-optimal rest-to-rest motion. First, an equilibrium equation was derived for a single-mass rigid-body mechanism subject to variable inertia $J(\theta)$ using the work-energy principle. Based on this equilibrium, a single equation was obtained to determine the optimal switching point θ_{SwP} in the angular domain. The optimum appears to depend only on the motor torque T_{motor} and load torque $T_l(\theta)$ along the trajectory and is, therefore, inertia $J(\theta)$ independent. Simulation results confirm that the single-mass switching point θ_{SwP} equation results in perfect rest-to-rest motion when friction and other secondary effects are neglected. Next, a corresponding control structure was proposed consisting of a pure torque controller followed by a cascade control. A simple self-learning mechanism was added to structurally correct residual errors caused by, e.g. model inaccuracies. For each new motion cycle $i + 1$, this mechanism updates the switching point $\theta_{SwP;i+1}$ employing the observed machine behavior of the previous cycle i . To demonstrate the effectiveness of the proposed control structure, it was implemented in simulation and subjected to a two-mass spring-damper system with friction. Results show that the initially obtained switching point $\theta_{SwP;i=1}$ can be used as an efficient starting point to determine the actual in-situ optimal switching point $\theta_{SwP;Opt}$. Finally, the self-learning control structure succeeds in finding the in-situ optimal switching point $\theta_{SwP;Opt}$, thus minimizing the motion time.

REFERENCES

- [1] N. V. Oosterwyck, F. Vanbecelaere, M. Haemers, D. Ceulemans, K. Stockman, and S. Derammelaere, "CAD Enabled Trajectory Optimization and Accurate Motion Control for Repetitive Tasks." IEEE 15th International Conference on Control and Automation, 2019.
- [2] M. Pellicciari, G. Berselli, and F. Balugani, "On Designing Optimal Trajectories for Servo-Actuated Mechanisms: Detailed Virtual Prototyping and Experimental Evaluation," *IEEE/ASME Transactions on Mechatronics*, vol. 20, no. 5, pp. 2039–2052, 2015.
- [3] D. Richiedei and A. Trevisani, "Analytical computation of the energy-efficient optimal planning in rest-to-rest motion of constant inertia systems," *Mechatronics*, vol. 39, pp. 147–159, 2016.
- [4] A. Dhanda and G. Franklin, "Real-time generation of time-optimal commands for rest-to-rest motion of flexible systems," *IEEE Transactions on Control Systems Technology*, vol. 21, no. 3, pp. 958–963, 2013.
- [5] C. A. Desoer and J. Wing, "An optimal strategy for a saturating sampled-data system," *IRE Transactions on Automatic Control*, vol. AC-6, no. 1, pp. 5–15, 1961.
- [6] L. Consolini and A. Piazzi, "Generalized bang-bang control for feed-forward constrained regulation," in *IEEE Conference on Decision & Control*, vol. 45, no. 10. IEEE, 2006, pp. 2234–2243.
- [7] L. Y. Pao, "Minimum-time control characteristics of flexible structures," *Journal of Guidance, Control, and Dynamics*, vol. 19, no. 1, pp. 123–129, 1996.
- [8] R. H. Brown, Z. Yan, and F. Xin, "Time-optimal acceleration control and point-to-point control of step motors," no. 1, pp. 593–596, 1990.
- [9] S. LaValle, "A bang-bang approach for time optimality," 2020. [Online]. Available: <http://lavalle.pl/planning/node794.html>
- [10] L. V. D. Broeck, M. Diehl, and J. Swevers, "Mechatronics A model predictive control approach for time optimal point-to-point motion control," vol. 21, pp. 1203–1212, 2011.

- [11] R. Verschuere, H. J. Ferreau, A. Zanarini, M. Mercang, and M. Diehl, "A Stabilizing Nonlinear Model Predictive Control Scheme for Time-optimal Point-to-point Motions," no. Cdc, pp. 2525–2530, 2017.
- [12] P. Janssens, G. Pipeleers, and J. Swevers, "Model-free iterative learning of time-optimal point-to-point motions for LTI systems," pp. 6031–6036, 2011.
- [13] N. V. Oosterwyck, F. Vanbecelaere, F. Knaepkens, M. Monte, K. Stockman, A. Cuyt, and S. Derammelaere, "Energy optimal motion profile optimization," 2022. [Online]. Available: [arXiv:2201.01595](https://arxiv.org/abs/2201.01595).
- [14] H. Dresig and F. Holzweißig, *Dynamics of Machinery*. Springer, 1967.
- [15] G. Also, "Lecture L22 - 2D Rigid Body Dynamics: Work and Energy," pp. 1–11, 2008.
- [16] "Work (Physics)." [Online]. Available: [https://en.wikipedia.org/wiki/Work_\(physics\)](https://en.wikipedia.org/wiki/Work_(physics))
- [17] S. R. Garces, A. B. Yahya, N. van Oosterwyck, D. Jacques, and S. Derammelaere, "Bode-based speed proportional integral and notch filter tuning of a permanent magnet synchronous machine driven flexible system," 2022. [Online]. Available: [arXiv:2202.08648](https://arxiv.org/abs/2202.08648).
- [18] Siemens Digital Industries, "Drive Optimization Guide," 2021. [Online]. Available: <https://support.industry.siemens.com/cs/document/60593549/drive-optimization-guide?dti=0\&pnid=14507\&lc=en-WW>
- [19] D. Lee and C. W. Ha, "Optimization process for polynomial motion profiles to achieve fast movement with low vibration," *IEEE Transactions on Control Systems Technology*, vol. 28, no. 5, pp. 1892–1901, 2020.

APPENDIX I

An equilibrium equation is derived for a single-mass system with variable inertia starting from the work-energy principle. Given the considered system, the work done can be described following:

$$\begin{aligned}
 & \int_{t_1}^{t_2} \left(T(t) \cdot \omega(t) \right) dt \\
 &= \int_{t_1}^{t_2} \left(\left(J(\theta) \cdot \alpha(t) + \frac{1}{2} \frac{d(J(\theta(t)))}{d(\theta(t))} \cdot \omega^2(t) \right) \cdot \omega(t) \right) dt \\
 &= \int_{t_1}^{t_2} \left(J(\theta) \cdot \alpha(t) \cdot \omega(t) \right) dt + \int_{t_1}^{t_2} \left(\frac{1}{2} \frac{d(J(\theta(t)))}{d(\theta(t))} \cdot \omega^3(t) \right) dt.
 \end{aligned} \tag{I.1}$$

Furthermore, we know that

$$\begin{aligned}
 \alpha(t) \cdot \omega(t) &= \omega(t) \cdot \frac{d\omega(t)}{dt} = \frac{1}{2} \cdot \left(\omega(t) \cdot \frac{d\omega(t)}{dt} + \omega(t) \cdot \frac{d\omega(t)}{dt} \right) \\
 &= \frac{1}{2} \cdot \frac{d(\omega(t) \cdot \omega(t))}{dt} = \frac{1}{2} \cdot \frac{d(\omega^2(t))}{dt}.
 \end{aligned} \tag{I.2}$$

And we also know that

$$\begin{aligned}
 \frac{1}{2} \frac{d(J(\theta(t)))}{d(\theta(t))} \cdot \omega^2(t) &= \frac{1}{2} \frac{d(J(\theta(t)))}{d(\theta(t))} \cdot \frac{d(\theta(t))}{dt} \cdot \omega(t) \\
 &= \frac{1}{2} \frac{d(J(\theta(t)))}{dt} \cdot \omega(t).
 \end{aligned} \tag{I.3}$$

Hence it follows from the substitution of (I.2) and (I.3) in (4) that

$$\begin{aligned}
 & \int_{t_1}^{t_2} \left(J(\theta(t)) \cdot \alpha(t) \cdot \omega(t) \right) dt + \int_{t_1}^{t_2} \left(\frac{1}{2} \frac{d(J(\theta(t)))}{dt} \cdot \omega^3(t) \right) dt \\
 &= \frac{1}{2} \int_{t_1}^{t_2} \left(J(\theta(t)) \cdot \frac{d(\omega^2(t))}{dt} \right) dt + \frac{1}{2} \int_{t_1}^{t_2} \left(\frac{d(J(\theta(t)))}{dt} \cdot \omega^2(t) \right) dt \\
 &= \frac{1}{2} \int_{\omega^2(t_1)}^{\omega^2(t_2)} \left(J(\theta(t)) \right) d(\omega^2(t)) + \frac{1}{2} \int_{J(\theta(t_1))}^{J(\theta(t_2))} \left(\omega^2(t) \right) d(J(\theta(t))).
 \end{aligned} \tag{I.4}$$

given that between time t_1 and t_2 the speed evolves along the $\omega(t_1)$ to $\omega(t_2)$ trajectory and the inertia along the $J(t_1)$

to $J(t_2)$ trajectory. By applying partial integration, the right term of (I.4) can be rewritten as

$$\begin{aligned} & \frac{1}{2} \int_{J(\theta(t_1))}^{J(\theta(t_2))} (\omega^2(t)) d(J(\theta(t))) \\ &= \frac{1}{2} \left[J(\theta(t)) \cdot \omega(t) \right]_{t_1}^{t_2} - \frac{1}{2} \int_{\omega^2(t_1)}^{\omega^2(t_2)} (J(\theta(t))) d(\omega^2(t)). \end{aligned} \quad (\text{I.5})$$

So that eventually, by combining (I.4) and (I.5), the total work W is equal to

$$\begin{aligned} W &= \frac{1}{2} \int_{\omega^2(t_1)}^{\omega^2(t_2)} (J(\theta(t))) d(\omega^2(t)) + \frac{1}{2} \left[J(\theta(t)) \cdot \omega(t) \right]_{t_1}^{t_2} \\ &\quad - \frac{1}{2} \int_{\omega^2(t_1)}^{\omega^2(t_2)} (J(\theta(t))) d(\omega^2(t)) \\ &= \frac{1}{2} \left[J(\theta(t)) \cdot \omega(t) \right]_{t_1}^{t_2} \\ &= \frac{J(\theta(t_2)) \cdot \omega(t_2)}{2} - \frac{J(\theta(t_1)) \cdot \omega(t_1)}{2}. \end{aligned} \quad (\text{I.6})$$

APPENDIX II

Derivation of the optimal switching point formula starting from the equilibrium equation (7).

$$\begin{aligned} 0 &= \int_P (T(\theta(t))) d(\theta(t)) \\ &= \int_{\theta_{start}}^{\theta_{SwP;Opt}} (T_{max}(\theta) - T_l(\theta)) d(\theta) \\ &\quad + \int_{\theta_{SwP;Opt}}^{\theta_{end}} (-T_{max}(\theta) - T_l(\theta)) d(\theta) \\ &= \int_{\theta_{start}}^{\theta_{SwP;Opt}} (T_{max}(\theta)) d(\theta) + \int_{\theta_{SwP;Opt}}^{\theta_{end}} (-T_{max}(\theta)) d(\theta) \\ &\quad + \int_{\theta_{start}}^{\theta_{end}} (-T_l(\theta)) d(\theta) \\ &= [T_{max} \cdot \theta]_{\theta_{start}}^{\theta_{SwP;Opt}} - [T_{max} \cdot \theta]_{\theta_{start}}^{\theta_{end}} - \int_{\theta_{start}}^{\theta_{end}} (T_l(\theta)) d(\theta) \end{aligned} \quad (\text{II.1})$$

$$\theta_{SwP;Opt} = \frac{T_{max} \cdot (\theta_{start} + \theta_{end}) + \int_{\theta_{start}}^{\theta_{end}} (T_l(\theta)) d(\theta)}{2 \cdot T_{max}} \quad (\text{II.2})$$